

Extremely Low Threshold 1.3- μm InAsP n-Type Modulation Doped MQW Lasers

by Hitoshi Shimizu*, Kouji Kumada*, Nobumitsu Yamanaka*,
Norihiro Iwai*, Tomokazu Mukaiharu* and Akihiko Kasukawa*

ABSTRACT A semiconductor laser with a low threshold current emitting at 1.3 μm wavelength is a key component for access networks and high-density parallel optical interconnections. A very low CW threshold current of 0.9 mA has been obtained at room temperature for lasers grown by gas-source molecular-beam epitaxy, which is the lowest value grown by any kind of molecular-beam epitaxy in the long wavelength region. Both the reduction of the threshold current and the carrier lifetime lead to the reduction of the turn-on delay time by about 30%. The 1.3 μm InAsP strained MQW lasers using n-type modulation doping with very low power consumption and small turn-on delay time are very attractive for laser array application in high density parallel optical interconnection systems.

1. INTRODUCTION

A semiconductor laser with a low threshold current emitting at 1.3 μm wavelength is a key device for access networks and high-density parallel optical interconnections. The strained-layer quantum well (SL-QW) lasers have an improved laser performance, such as low threshold current, high output power, high relaxation oscillation frequency and so on. These improvements result from low internal loss and high differential gain due to the change of valence band structure¹⁾. So far, GaInAsP/InP material systems have been used in 1.3 μm SL-QW lasers for optical communication systems. On the other hand, InAsP/InP system is another candidate for this wavelength^{2), 3)}. The large conduction band offset of $\Delta E_c=0.7 \Delta E_g$ reported for this material system⁴⁾ makes it possible to realize a strong electron confinement in the wells, which is expected to result in a lower threshold current, higher differential gain and higher characteristic temperature (T_0). However, in order to adjust the wavelength to 1.3 μm range, InAsP wells have to have a large compressive strain ($\epsilon=1.4\sim 1.6\%$), therefore gas-source molecular-beam epitaxy (GSMBE) is favorable as the growth method of InAsP material because the low temperature growth of GSMBE increases the critical thickness.

On the other hand, modulation doped MQW (MD-MQW) laser, which consists of undoped wells and doped barriers, has been proposed for further improvement of the laser performance⁵⁾. So far, low threshold lasers have been reported for n-type MD-MQW lasers grown by both MOCVD (Se-dope)^{6), 7)} and GSMBE (Si-dope)^{8), 9)}. Optical

gain g is proportional to $(f_c - f_v)$, where f_c (f_v) is Fermi-Dirac function for electrons (holes). This term can be divided into two terms, which are expressed as

$$g \sim (f_c - f_v) = f_c(1 - f_v) - f_v(1 - f_c) \quad \dots(1)$$

Here, the first term $f_c(1 - f_v)$ shows the stimulated emission term and the second term shows the stimulated absorption term. As f_c approaches unity with respect to n-type MD-MQW laser, the absorption term becomes zero, which leads to low threshold current density. However, the doping profile needs to be sharp in this structure. Due to these points, we think that GSMBE is a suitable growth method for this type of laser.

In this paper, we investigate systematically the effect of n-type modulation doping on the characteristics of 1.3 μm InAsP MQW lasers grown by GSMBE for the first time. In section 2, we discuss the structure of n-type MD-MQW lasers and the results of the threshold current densities. In section 3, we discuss fabrication of ridge lasers and extract the basic laser parameters such as gain coefficient, internal loss, and characteristic temperature of n-type MD-MQW laser and undoped MQW laser. In section 4, we present fabrication of buried heterostructure (BH) lasers and show the excellent performance of the n-type modulation doped MQW lasers.

2. FABRICATION OF MQW LASERS AND EVALUATION OF BASIC MATERIAL QUALITY

We have grown 1.3 μm InAsP/GaInAsP MQW lasers on n-InP substrates by GSMBE in which group III is the solid source and group V is AsH₃ and PH₃ and the dopant is Si

* Semiconductor R&D Center, Yokohama R&D Laboratories, R & D Div.

for n-type and Be for p-type. As shown in Figure 1, the lasers consisted of n-, p-InP cladding, compressively strained MQW active layer, and 120 nm thick GaInAsP SCH layer ($\lambda_g=1.1 \mu\text{m}$) located on both sides of MQW. The MQW active region consists of 1.45% compressively strained three InAs_{0.45}P_{0.55} quantum wells (each 8 nm thick) separated by lattice-matched GaInAsP barrier layers (each 10 nm thick) of the same composition as SCH. The 7 nm thick center region of each barrier layer is doped with silicon. The optimum growth temperature is 515°C for InP cladding layer and 455°C for SCH-MQW layer and the optimum modulation doping density was $1 \times 10^{18} \text{ cm}^{-3}$ as described in another paper^{8),10)}.

Figure 2 shows the dependence of J_{th} on inverse cavity length for undoped MQW lasers and MD-MQW lasers ($N_D=1 \times 10^{18} \text{ cm}^{-3}$) grown at optimum growth condition. The threshold current density at an infinite cavity $J_{th\infty}$ was reduced by about 30% as compared with undoped MQW lasers and the extremely low threshold current density of 250 A/cm² was obtained for 1200 nm-long MD-MQW lasers. The threshold current density per well was comparable to the previously reported n-type MD-MQW lasers grown by MOCVD^{6),7)}. The reduction of J_{th} of MD-MQW laser could be due to the reduction of the threshold carrier density caused by the reduction of the transparent carrier density^{5),6)}.

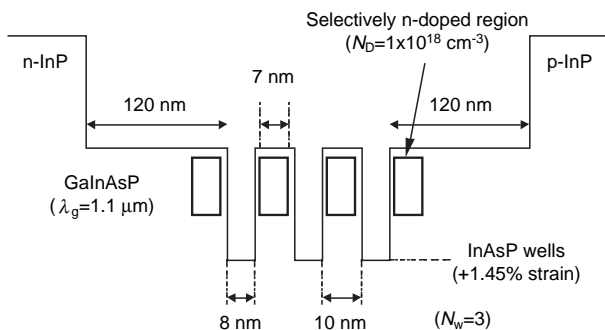


Figure 1 Schematic band diagram of 1.3 μm InAsP/GaInAsP n-type MD-MQW lasers

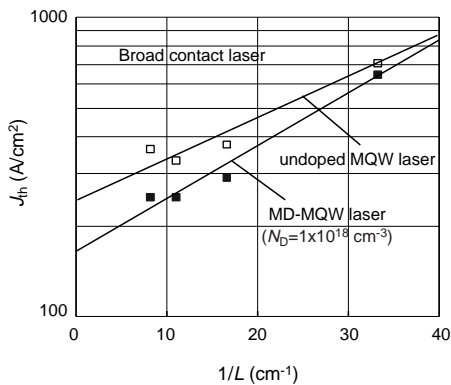


Figure 2 J_{th} dependence of on inverse cavity length in undoped MQW lasers and MD-MQW

3. LASING CHARACTERISTICS OF RIDGE LASERS

For the estimation of the laser characteristics, we fabricated ridge-lasers with 20 μm width for MD-MQW lasers (N_D of $1 \times 10^{18} \text{ cm}^{-3}$) and undoped MQW lasers. To fabricate ridge waveguide, p⁺-GaInAs contact layer and p-InP cladding layer were removed by conventional wet chemical etching with stripe geometry oxide mask.

The external differential quantum efficiency η_d is associated to the internal loss α_i and the internal efficiency η_i , which is determined by the product of internal quantum efficiency and current injection efficiency, as

$$\frac{1}{\eta_d} = \frac{1}{\eta_i} \left(1 + \frac{\alpha_i L}{\ln(1/R)} \right) \quad \dots(2)$$

where: L is the cavity length and R is the average facet reflectivity.

Figure 3 shows the inverse external differential quantum efficiency versus cavity length for devices with cleaved facets. From the relationship in (2), α_i and η_i were estimated. The obtained internal efficiencies were almost 100% for both types of lasers, and the internal loss was 6.0 cm^{-1} for the undoped laser and 4.6 cm^{-1} for MD-MQW laser. The reduction of internal loss of MD-MQW laser was explained by the reduction of intervalence band absorption loss caused by the reduction of the threshold carrier densities⁶⁾. Semilogarithmic approximation for optical gain g per well is given by

$$g = G_0 \ln \left(\frac{\eta_i J}{N_w J_{tr}} \right) \quad \dots(3)$$

where: J is the injected current density, J_{tr} is the transparent current density, and G_0 is the gain coefficient.

J_{th} can be then expressed as follows.

$$J_{th} = \frac{N_w J_{tr}}{\eta_i} \exp \left\{ \frac{1}{N_w \Gamma_w G_0} (\alpha_i + \alpha_m) \right\} \quad \dots(4)$$

where: Γ_w and α_m denote the optical confinement factor per well and mirror loss, respectively.

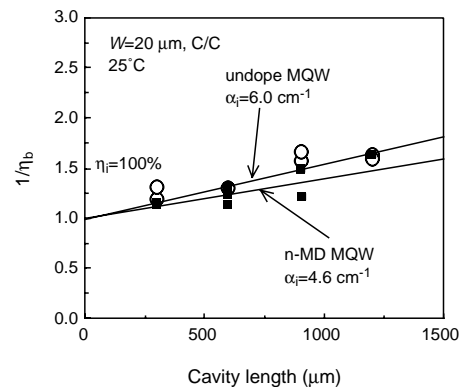


Figure 3 Inverse differential quantum efficiency versus cavity length for ridge lasers with 20 μm width

The optical confinement factor per well is theoretically estimated by solving the Maxwell's equation for multilayer waveguide with TE mode, which is 0.0149 per well. G_0 estimated from the results of ridge lasers was 720 cm^{-1} for undoped MQW lasers and 650 cm^{-1} for MD-MQW lasers, which indicates that G_0 does not decrease significantly by using n-type MD-MQW lasers. The value of G_0 for undoped MQW lasers is comparable to the previously reported value on undoped InAsP MQW laser ($N_w=3$).

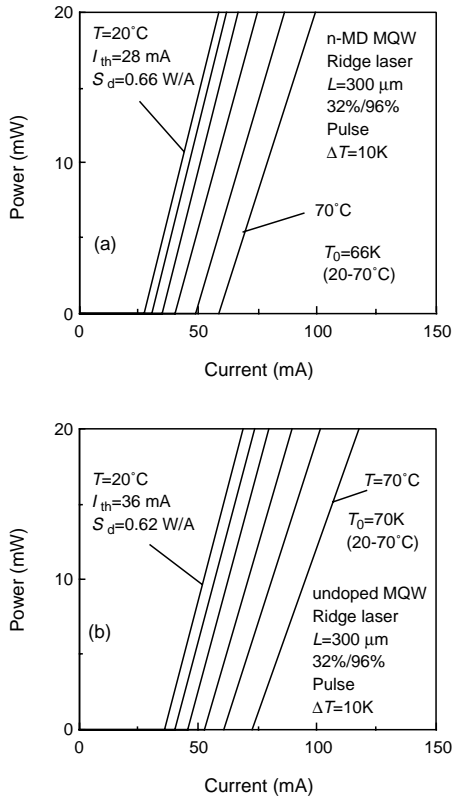


Figure 4 Temperature dependence of light output versus current characteristics at pulse operation for MD-MQW ridge laser (a) and undoped MQW ridge laser (b) with $300 \mu\text{m}$ -long cavity and $20 \mu\text{m}$ width (cleaved front facet, $R_f=R_r=96\%$ coated)

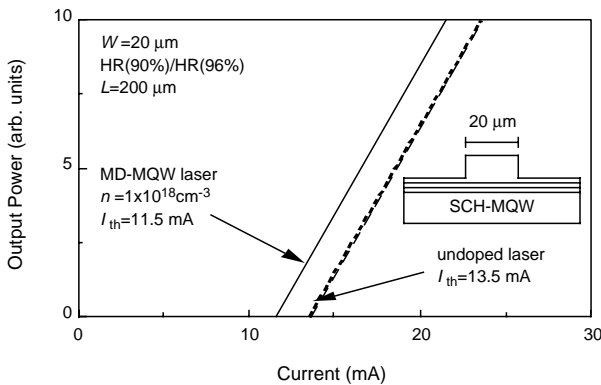


Figure 5 Light output versus current characteristics of MD-MQW ridge laser ($N_D=1 \times 10^{18} \text{ cm}^{-3}$) and undoped MQW ridge laser with $20 \mu\text{m}$ -width and $200 \mu\text{m}$ -long cavity ($R_f=90\%$, $R_r=96\%$ coated). The inset shows the schematic sectional plan of ridge lasers.

The temperature dependence of light output power versus injected current characteristics for ridge lasers were investigated. Figure 4 shows the temperature dependence of output power versus current characteristics at pulse operation for MD-MQW lasers and undoped MQW lasers on $300 \mu\text{m}$ -long device with high reflective coatings (96%) on the rear facet. The threshold current of MD-MQW lasers was as low as 28 mA at 20°C and was reduced by about 20% as compared with undoped MQW laser. The obtained slope efficiency was as high as 0.66 W/A for MD-MQW laser, and that of undoped MQW laser was 0.62 W/A. The characteristic temperature T_0 was 66 K for MD-MQW and 70 K for undoped MQW laser in the range of 20°C to 70°C . No significant degradation of T_0 was observed for MD-MQW laser as compared with undoped MQW lasers, which agrees with the results of G_0 .

To reduce the threshold current of ridge lasers, we fabricated short cavity lasers with high reflection (HR) coatings on both facets ($R_f/R_r=90\%/96\%$), because J_{th} of n-type MD-MQW laser becomes very low at the low mirror loss region. As shown in Figure 5, a very low threshold current of 11.5 mA was obtained for MD-MQW lasers with $200 \mu\text{m}$ -long cavity although the width of ridge lasers were $20 \mu\text{m}$, from which we can expect submilliampere levels for the threshold current if we fabricate $1.5 \mu\text{m}$ -wide BH lasers.

4. LASING CHARACTERISTICS OF BH LASERS

Buried heterostructure (BH) lasers with p- and n-InP blocking layers were fabricated for the GSMBE-grown MD-MQW epitaxial wafers ($N_D=1 \times 10^{18} \text{ cm}^{-3}$) by MOCVD as shown in Figure 6. The typical width of the active region W is $1.6 \mu\text{m}$. The trench structure was fabricated to reduce the leakage current and the intrinsic capacitance.

The cavity length dependence of the threshold currents as a parameter of the facet reflectivity for MD-MQW lasers ($N_D=1 \times 10^{18} \text{ cm}^{-3}$) under room-temperature pulsed condition is shown in Figure 7. The lines are theoretical values which are calculated by the following equation using the parameters extracted from the threshold characteristics of the ridge lasers mentioned in section 3.

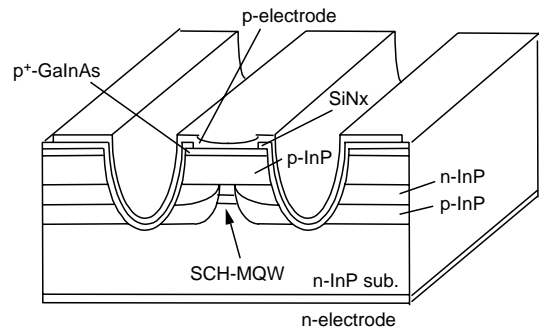


Figure 6 Schematic diagram of $1.3\text{-}\mu\text{m}$ InAsP MQW buried hetero-structure lasers

$$I_{th} = WL \frac{N_w J_{tr}}{\eta_i} \exp\left\{ \frac{1}{N_w \Gamma_w \Gamma_l G_0} \left(\alpha_i + \frac{1}{2L} \right) \ln\left(\frac{1}{R_f R_r} \right) \right\} \dots(5)$$

where: Γ_l is the lateral confinement factor and R_f (R_r) is the reflectivity on the front (rear) facet. Γ_l was assumed to be unity because Γ_w and W are relatively large.

Open circles, crosses, and squares show the experimental results of lasers with cleaved facets, 32%/96%, and 90%/96%, respectively. The averaged threshold currents of 300 μm , 600 μm and 900 μm long devices with cleaved facets were 7 mA, 6.3 mA, and 7.5 mA, respectively. The threshold currents for devices with short cavity and HR coating agree with calculations, on the other hand, discrepancies between calculations and experiments are observed at the large mirror loss region and the long cavity region. The discrepancies are considered to be leakage current due to imperfect current blocking in the buried heterostructure, which becomes larger in devices with longer cavity and higher threshold current density.

A CW light output power versus current characteristics at 25°C is shown in Figure 8 for a 150 μm -long device with HR coatings of $R_f/R_r=90\%/96\%$ along with the inset of lasing spectrum operating at 2 mA. A very low CW

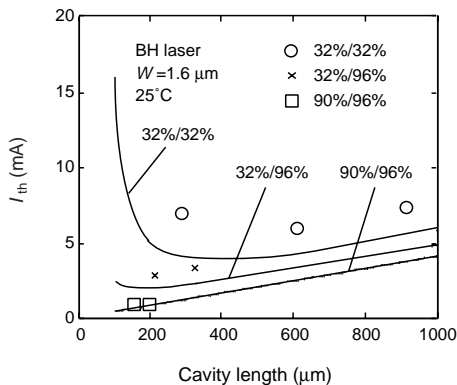


Figure 7 Threshold current versus cavity length of MD-MQW BH lasers ($N_D=1 \times 10^{18} \text{cm}^{-3}$) with facet reflectivity as a parameter

threshold current of 0.9 mA, corresponding to the threshold current density of 375 A/cm², was obtained even though the laser is not bonded on a heat sink. So far, a few studies have been done on submilliampere operation in 1.3 μm range at room temperature (0.4 mA¹¹), 0.58 mA¹², 0.98 mA¹³, 0.80 mA¹⁴), and all of those were grown by MOCVD using strained quantum well layers. This is the lowest value ever reported for long wavelength lasers using n-type modulation doping⁶) and the lowest grown by any kind of MBE in the long wavelength³) to our best knowledge. Note that a lower threshold current can be expected in a device with shorter cavity and narrower stripe width.

The temperature dependence of light output power versus injected current characteristics for BH lasers with MD-MQW ($N_D=1 \times 10^{18} \text{cm}^{-3}$) were investigated. Figure 9 shows the temperature dependence of output power versus current characteristics at DC operation for MD-MQW lasers on 300 μm -long device with HR coating (96%) on the rear facet. The threshold current at 20°C was as low as 3.2 mA and the slope efficiency was as high as 0.70 W/A. The threshold current at 70°C was 8.8 mA and the slope efficiency was 0.57 W/A. The characteristic temperature was 48 K in the range of 20°C to 70°C. This low T_0 value compared with the results of ridge lasers is probably

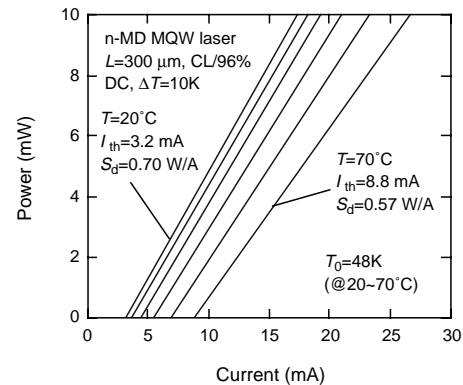


Figure 9 Temperature dependence of output power versus current characteristics for MD-MQW BH laser with 300 μm -long cavity (cleaved front facet, $R_r=96\%$ coated) under DC operation

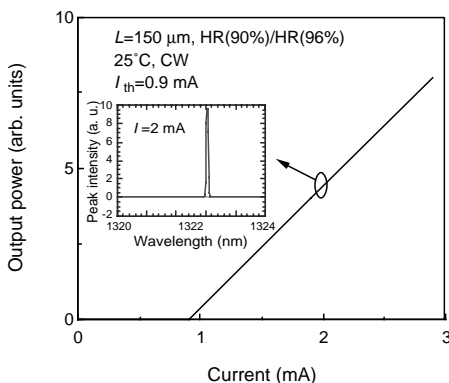


Figure 8 Light output power versus current characteristics of 150 μm -long MD-MQW BH lasers with HR coatings ($R_f/R_r=90\%/96\%$) with the inset of the lasing spectrum operating at 2 mA

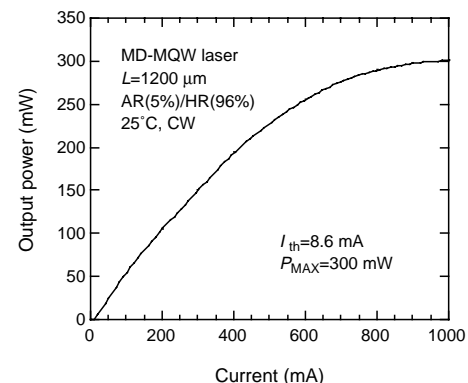


Figure 10 Light output power versus current characteristics of 1200 μm -long MD-MQW BH lasers with AR/HR coated facets ($R_f=5\%$, $R_r=96\%$ coated)

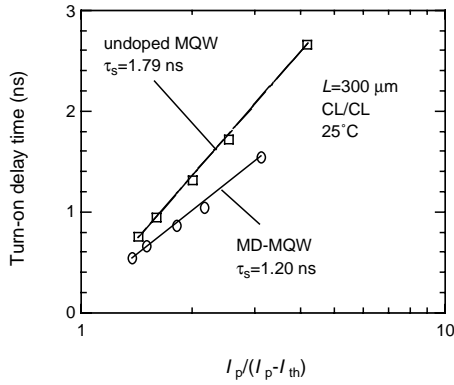


Figure 11 Turn-on delay time versus normalized bias level $I_p/(I_p - I_{th})$ for MD-MQW BH laser and undoped MQW BH laser with 300 μm -long cavity and cleaved facets. The lasers were zero-biased

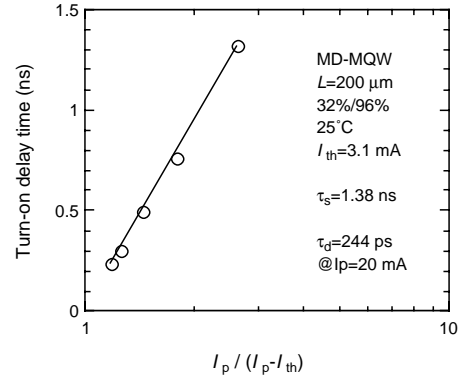


Figure 13 Turn-on delay time versus normalized bias level $I_p/(I_p - I_{th})$ for MD-MQW BH laser of 200 μm -long cavity (cleaved front facet, $R_r=96\%$ coated). The lasers were zero-biased

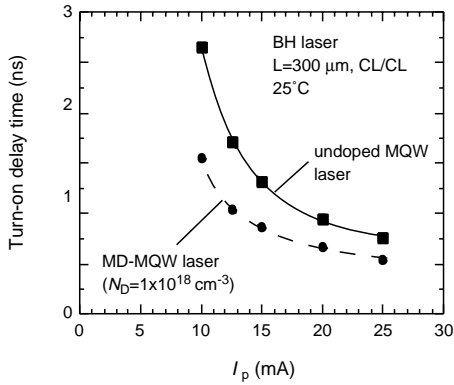


Figure 12 Turn-on delay time versus height of pulse current for MD-MQW BH lasers and undoped MQW BH lasers with 300 μm -long cavity and cleaved facets. The lasers were zero-biased

governed by the T_0 of leakage current in the blocking layer.

Further, we evaluated high output power characteristics of MD-MQW lasers because internal loss of MD-MQW lasers becomes smaller than that of undoped MQW lasers. Figure 10 shows the light output power versus injected current characteristics of 1200 μm -long MD-MQW laser with AR coating (5%) on the front facet and HR coating (96%) on the rear facet. The lasers were operated under DC operation at 25°C. The threshold current was 8.6 mA and the obtained maximum output power was 300 mW. The saturation of output power was probably limited by the increase of the temperature of the active region. The FWHM of the far-field patterns (FFP's) parallel and perpendicular to the junction plane at output power of 100 mW were 22° and 32°, respectively.

The other advantage of low threshold lasers is to decrease the skew in laser array. The turn-on delay time of the semiconductor laser under zero-bias operation is affected by its threshold current as ⁽¹⁵⁾

$$\tau_d = \tau_s \ln \{ I_p / (I_p - I_{th}) \} \quad \dots (6)$$

where: I_p is the height of the pulse current and τ_s is the carrier lifetime.

N-type MD-MQW lasers have been predicted to decrease the carrier lifetime because of their higher total spontaneous emission rate with the increased doping density, which results in further reduction of turn-on delay time. All measurements were carried out under zero-bias condition at 25°C. Figure 11 shows the relationship between the turn-on delay time and the normalized bias level $I_p/(I_p - I_{th})$ for MD-MQW BH laser and undoped MQW BH laser with 300 μm -long cavity and cleaved facets. The carrier lifetimes of 1.79 ns for undoped MQW and 1.20 ns for MD-MQW lasers were estimated from the slope in Figure 11. The carrier lifetimes were reduced by about 33%. The reduction of both the threshold current and the carrier lifetime using n-type MD-MQW leads to the reduction of the turn-on delay time ⁽⁶⁾.

Figure 12 shows the relationship between turn-on delay time and the height of the pulse current I_p for MD-MQW BH lasers and undoped MQW BH lasers. The turn-on delay time of MD-MQW laser was reduced by about 30% as compared with undoped MQW lasers at the height of a pulse current of 20 mA.

Figure 13 shows the relationship between the turn-on delay time and the normalized bias level $I_p/(I_p - I_{th})$ for MD-MQW BH laser of 200 μm -long cavity with HR coating (96%) on the rear facet. The threshold current was 3.1 mA at 25°C and the lasers were zero-biased. The obtained turn-on delay time was 244 ps at a pulse current height of 20 mA.

The 1.3 μm InAsP strained MQW lasers using n-type modulation doping with very low power consumption and small turn-on delay time grown by gas-source MBE are very attractive for laser array application in high density parallel optical interconnection systems.

5. CONCLUSIONS

We investigated the effect of n-type modulation doping on the performance of 1.3 μm InAsP strained MQW lasers grown by gas-source MBE. A very low CW threshold current of 0.9 mA has been obtained in 1.3 μm InAsP n-type modulation doped MQW laser, at room temperature, which is the lowest grown value among all kinds of molecular beam epitaxy in the long wavelength region. The carrier lifetime was also reduced by about 33% by using n-type MD-MQW lasers. Both the reduction of the threshold current and the carrier lifetime caused the reduction of the turn-on delay time by about 30%. The high power performance of MD-MQW lasers was also demonstrated. We confirmed the low threshold current, the high efficiency and the short turn-on delay time by using n-type modulation doped MQW lasers.

ACKNOWLEDGMENTS

The authors would like to thank Mr. J. Kikawa and Mr. T. Ninomiya for their encouragement throughout this study. We also acknowledge Dr. N. Yokouchi for his assistance in the theory of x-ray simulation and the calculation of the optical confinement factors. Further, we acknowledge Dr. S. Yoshida, Dr. Y. Hiratani, and Dr. J. Yoshida for helpful discussions on GSMBE growth.

REFERENCES

- 1) R. Adams: *Electron. Lett.* 22 (1986) 249-250.
- 2) Kasukawa et al.: *IEEE J. Quantum Electron.* 29 (1993) 1528.,
- 3) P. Thiagarajan et al.: *J. Cryst. Growth* 175 (1997) 945.
- 4) R. P. Schneider et al.: *J. Electron. Mater.* 20 (1991) 1117.
- 5) K. Uomi : *Jpn. J. Appl. Phys.* 29 (1990) 81.
- 6) K. Nakahara et al.: *IEEE J. Select. Topics in Quantum Electron.* 3 (1997) 166.
- 7) T. Yamamoto et al.: *IEEE Photon. Technol. Lett.* 6 (1994) 1165.
- 8) H. Shimizu et al.: *Electron. Lett.* 34 (1998) 888.
- 9) H. Shimizu et al.: *Electron. Lett.* 34 (1998) 1591.
- 10) H. Shimizu et al.: *Furukawa Review* No. 18 (1999) 61.
- 11) T. Terakado et al.: *Electron. Lett.* 31 (1995) 2182.
- 12) K. Uomi et al.: *IEEE J. Select. Topics Quantum Electron.* 1 (1995) 203.
- 13) E. Zah et al.: *IEEE J. Quantum Electron.* 27 (1991) 1440.
- 14) J. S. Osinski et al.: *IEEE Photon. Technol. Lett.* 4 (1992) 1313.
- 15) N. K. Dutta et al.: *Appl. Phys. Lett.* 61 (1992) 130.

Manuscript received on July 2, 1999.